Institute of Space and Aeronautical Science, University of Tokyo
Report No. 591, February 1981

Inlet Distortion and Blade Vibration in Turbomachines

By

Yoshimichi TANIDA and Toshio NAGASHIMA

Abstract: Nonuniformity of inlet flows through a test compressor stage has been studied based upon 3-D semi-actuator disk theory. The results show that the rotor blade vibration greatly influences the attenuation rate of distortion. The effects of the rotor/stator separation, the circumferential modal index and the tilting of the inlet distortion, are also demonstrated.

1. INTRODUCTION

In the theoretical treatment of nonuniform inlet flows, the assumption of plane type disturbances is commonly made, [*1*], so that the distortion or vorticity interacting with cascades is always directed parallel to the blade span. When the spanwise variation of the inlet nonuniformity is apparently present in flow, however, the extension of the theory for disturbances in three dimensions needs to be developed. Yeh's actuator disc analysis [*2*] and the comment on it by Dunham [*3*] were the first among such attempts. In Yeh's model the inertial effects of the fluid inside the blade passages are not taken into account, nor the distortion-induced vibration of rotor blades. These short-comings can be overcome by introducing the concept of the semi-actuator disc model [*4*]. In what follows, the earlier two dimensional semi-actuator model [*5*] is extended into the three dimensional disturbance model in uniform mean flow between parallel walls. The main restriction upon using it is that the wavelength of disturbances in the cascade direction be large compared with the blade spacing, which will be allowed for most of the circumstances appearing in the interaction problems between inlet distortion and cascade blades.

2. THEORY

Under the assumption of small perturbations upon compressible, isentropic, uniform mean flow, the equations of continuity, momentum and the isentropic flow relationship may be linearized. The coordinate system is taken as shown in Fig. 1, x being the machine axis and y, z axes directing to the cascade line and blade span, respectively. The fluid pressure, density and the flow velocity vector are expressed as p_0+p, $\rho_0+\rho$ and (V_x+v_x, V_y+v_y, v_z) in which p_0, ρ_0 and $(V_x, V_y, 0)$ are the values of the mean flow, while p, ρ, (v_x, v_y, v_z) are the corresponding perturbations. The sound speed C_0 is given by $\sqrt{\kappa p_0/\rho_0}$.

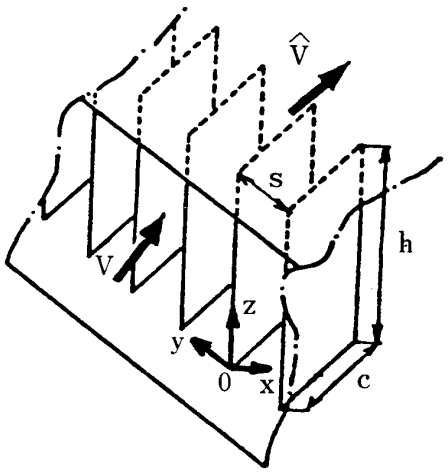

FIG. 1. Coordinate system

Perturbations Outside the Cascade:

Imposing the boundary condition that $v_z=0$ at $z=0$ and h, the required solutions, of propagating type in the cascade direction and with harmonic time dependence, can be derived as follows;

$$\begin{bmatrix} v_x \\ v_y \\ v_z \\ p/\rho_0 C_0 \\ \rho/\rho_0 \end{bmatrix} = \begin{bmatrix} -k_1/D_1 & -k_2/D_2 & i\omega/V_p & -\pi\nu/h \\ (i\omega/V_p)/D_1 & (i\omega/V_p)/D_2 & k_0 & 0 \\ (\pi\nu/h)/D_1 & (\pi\nu/h)/D_2 & 0 & k_0 \\ 1 & 1 & 0 & 0 \\ 1/C_0 & 1/C_0 & 0 & 0 \end{bmatrix} \cdot \begin{bmatrix} B_1 \cdot e^{k_1 \cdot x} \\ B_2 \cdot e^{k_2 \cdot x} \\ B_3 \cdot e^{k_0 \cdot x} \\ B_4 \cdot e^{k_0 \cdot x} \end{bmatrix} \cdot e^{i\omega(t-y/V_p)} \begin{matrix} \times\cos[(\pi\nu/h)z] \\ \times\cos[(\pi\nu/h)z] \\ \times\sin[(\pi\nu/h)z] \\ \times\cos[(\pi\nu/h)z] \\ \times\cos[(\pi\nu/h)z] \end{matrix} \quad (1)$$

where, ω is the angular frequency, V_p is the phase velocity of propagation in y-direction, and ν is the spanwise modal order ($\nu=0, 1, \cdots$). The last harmonic factor indicates the spanwise modal dependence corresponding to each flow parameter. In general the solution is given by the sum of contributions from all the spanwise modal components. The wave numbers k_0, k_1 and k_2 are given by $k_0=-i[\omega/V_x-(\omega/V_p)\cdot(V_y/V_x)]$, $k_1=(-M_x^2\cdot k_0+\sqrt{D_0})/\beta_x^2$, $k_2=(-M_x^2\cdot k_0-\sqrt{D_0})/\beta_x^2$ in which $D_0=\beta_x^2\cdot[(\omega/V_p)^2+(\pi\nu/h)^2]+M_x^2\cdot k_0^2$. B_1 and B_2 are the amplitudes of k_1- and k_2-pressure waves, while B_3 and B_4 are those of y- and z-components of velocity perturbation associated with the vortex waves. A part of these coefficients can be fixed a priori from the physical grounds, for instance, the outgoing wave condition requires that $B_1=0$ or $B_2=0$ at far down-or up-stream field, while the irrotational flow finds that $B_3=B_4=0$. The other symbols are defined as $D_1=M_x\cdot(k_1-k_0)$, $D_2=M_x\cdot(k_2-k_0)$, $\beta_x^2=1-M_x^2$ and $M_x=V_x/C_0$.

Cascade Field Perturbations:

In the semi-actuator disc model, the blade spacing s is assumed to be small compared with the wavelength of the disturbances, therefore the incident flow is squeezed to follow the interblade passage and the variation across its width will be neglected. A care must be noted, in cases when the blades are vibrating, that the relative movement between the neighbouring blades, however small the spacing is, should be taken into account. It is convenient to introduce the cascade coordinate system (ξ, η, z) attaching to the reference blade at a time in question and henceforth keeps its constant speed relative to the machine coordinates (x, y, z). The relationship of the perturbation velocity components between the two systems is that $v_\xi = v_x \cdot \cos\theta + v_y \cdot \sin\theta$, $q = -v_x \cdot \sin\theta + v_y \cdot \cos\theta$, in which q is the vibration velocity of blade surface and θ is the stagger angle of the cascade. The solution for the cascade field perturbations is written as

$$\begin{bmatrix} v_\xi \\ v_z \\ p/\rho_0 C_0 \\ \rho/\rho_0 \end{bmatrix} = \left(\begin{bmatrix} -k_1^*/D_1^* & -k_2^*/D_2^* & -\pi\nu/h \\ (\pi\nu/h)/D_1^* & (\pi\nu/h)/D_2^* & k_0^* \\ 1 & 1 & 0 \\ 1/C_0 & 1/C_0 & 0 \end{bmatrix} \cdot \begin{bmatrix} B_1^* \cdot e^{k_1^* \xi} \\ B_2^* \cdot e^{k_2^* \xi} \\ B_4^* \cdot e^{k_0^* \xi} \end{bmatrix} + \begin{bmatrix} 0 \\ -i(\pi\nu/h)/D^* \\ (\omega/C_0)/D^* \\ (\omega/C_0)/D^*/C_0 \end{bmatrix} \cdot (\omega/V_p)(q_0/\cos\theta) \right) \cdot e^{i\omega t} \qquad (2)$$

where, $k_0^* = -i\omega/V$, $k_1^* = (-M^2 \cdot k_0^* + \sqrt{D_0^*})/\beta^2$ and $k_2^* = (-M^2 \cdot k_0^* - \sqrt{D_0^*})/\beta^2$ with $D_0^* = \beta^2 \cdot (\pi\nu/h)^2 + M^2 \cdot k_0^{*2}$, $D_1^* = M \cdot (k_1^* - k_0^*)$, $D_2^* = M \cdot (k_2^* - k_0^*)$, $\beta^2 = 1 - M^2$, $M = V/C_0$ and $D^* = -(\pi\nu/h)^2 + (\omega/C_0)^2$. The coefficients B_1^*, B_2^* and B_4^*imply the pressure and vortex waves as before, but under the restriction of plane flow perturbations. The second term in the bracket represents the effect of the phase lag in the vibrating motion between adjacent blades. In the expression, the spanwise modal factors, corresponding to the cosine and sine multipliers of the equation (1), have been omitted.

Matching Conditions:

The solutions in the upstream, cascade and downstream flow fields are matched at the leading and trailing edges of the cascade by means of conservation laws of mass, momentum and total enthalpy. The matching conditions are derived as follows; at the leading edge,

$$<\rho_0 v_x + \rho V_x> - <\rho_0 (V_y - V_p)> \cdot q \sin\theta / V_p = 0 \qquad (3)$$

$$<p + 2\rho_0 V_x v_x + \rho V_x^2> - <\rho_0 V_x^2 + \rho_0 V_x V_y \tan\theta + p_0> \cdot q \cos\theta / V_p = -f_x/s \qquad (4)$$

$$<\rho_0 V_y v_x + \rho_0 V_x v_y + \rho V_x V_y> + <\rho_0 V_y \cdot (V_p \tan\theta - V_x - V_y \tan\theta) - p_0 \cdot \tan\theta> q \cos\theta / V_p = -f_y/s \qquad (5)$$

$$<\rho_0 V_x v_z> + <p_0 \cdot \sin\theta>(dq/dz)/i\omega = -f_z/s \quad (6)$$

$$<\rho_0 V_x^2 v_x + \rho_0 V_x V_y v_y + \rho V_x C_0^2> + <\rho_0 V_x^2 \cdot (\tan\theta - V_y/V_x)> \cdot q\cos\theta = 0 \quad (7)$$

while, at the trailing edge, assuming that the outlet flow leaves smoothly along the blade chord;

$$<v_x> = <v_y> = <v_z> = <p> = <\rho> = 0 \quad (8)$$

where, $<*>$ denotes the jump in the value of the quantity * across the matching plane and (f_x, f_y, f_z) is the singular unsteady forces at the leading edge. An additional condition is yet needed to match the number of unknowns and the equations being satisfied. From the physical ground it is assumed that the force vector acting upon the leading edge should be always normal to the instantaneous span inclination at the leading edge. That gives

$$<(p_0 + \rho_0 V_x^2)\sin\theta - \rho_0 V_x V_y \cos\theta>(dq/dz)/i\omega = -f_z/s \quad (9)$$

Bending Vibration of Blades:

The unsteady force L normal to the blade surface is derived from the momentum law and written as

$$\begin{aligned} L/\rho_0 V_x s = &<p\cdot\sin\theta/\rho_0 V_x + v_x\cdot\sin\theta - v_y\cdot\cos\theta> - (v_x + \rho/\rho_0\cdot V_x) \\ &\times(\sin\theta - V_y\cdot\cos\theta/V_x) + i(\omega c/V_p)\cdot(\tilde{p}/\rho_0 V_x) - [i(\omega c/\hat{V}_x)\cdot\cos\theta \\ &+ <V_y/V_x>\sin\theta\cdot\cos\theta - (V_x/V_p)\cdot(\sin\theta - V_y\cdot\cos\theta/V_x) \\ &\times(\cos\theta + V_y\cdot\sin\theta/V_x)]\cdot q \end{aligned} \quad (10)$$

where, $\tilde{p}$ is the unsteady pressure averaged over the interblade channel, and the superscript $\hat{}$ means the downstream quantities, otherwise the values are taken at the upstream field. This will be conveniently split into two parts, that being proportional to the vibration speed q and the remainder arising from the presence of inlet distortion, e.g. $L/\rho_0 V_x s = f_q\cdot q + f_{\bar{\omega}}\cdot\bar{\omega}$ in which $\bar{\omega}$ is the inlet vorticity and $q = \partial\varepsilon/\partial t$. ε is the vibration displacement and generally expressed as the superposition of normal bending modes, i.e.

$$\varepsilon(z;t) = \sum_{n=1}^{\infty}\varepsilon_n\cdot\psi_n(z)\cdot\exp[i\omega t] \quad (11)$$

The shape function ψ_n satisfies the equation

$$[d^2/dz^2(EI\cdot d^2/dz^2) - m\cdot\omega_n^2]\cdot\psi_n(z) = 0 \quad \text{with} \quad (2/h)\cdot\int_0^h \psi_n^2(z)\cdot dz = 1 \quad (12)$$

where, EI is the rigidity for bending motion, m is the blade mass and ω_n is the natural frequency corresponding to ψ_n normal mode being determined from the proper conditions at both ends along the span. Since the normal force L is obtained in the expression of the Fourier series expansion, i.e.

$$L/\rho_0 V_x s=\sum_{\nu=0}^{\infty}(f_{q\nu}\cdot q+f_{\bar{\omega}\nu}\cdot\bar{\omega})\cdot\cos[(\pi\nu/h)z] \tag{13}$$

it is convenient to write the displacement ε as

$$\varepsilon(z;t)=\sum_{\nu}\left(\sum_{n}\varepsilon_n\cdot\psi_{n\nu}\right)\cdot\cos[(\pi\nu/h)z]\cdot\exp[i\omega t] \tag{14}$$

where, $\psi_{n\nu}=(\varepsilon_\nu/h)\int_0^h\psi_n(z)\cdot\cos[(\pi\nu/h)z]\cdot dz$; $\varepsilon_\nu=1$ for $\nu=0$, and 2 for $\nu\neq0$. Substitution of these expressions into the equation of motion of blade vibration yields

$$\sum_{n}[\bar{m}\cdot(-\omega^2+\omega_n^2)/\omega^2+i\cdot\bar{m}\cdot\delta/\omega-i\cdot f_{q\nu}/(\omega c/V_x)]\varepsilon_n\psi_{n\nu}$$
$$=[V_x/(\omega c)]^2\cdot[f_{\bar{\omega}\nu}/(V_x/c)]\cdot\bar{\omega}_\nu \tag{15}$$

in which the mass ratio $\bar{m}$ is defined by $m/\rho_0 cs$ and δ is the mechanical damping coefficient. This shows that the ν-modal component of the inlet distortion induces all the coupled normal modes of vibration.

3. Application

Results from the theory are applied for a test compressor of rotor-stator stage (Fig. 2) with the tip/hub diameters 300 mm/200 mm and blade chord length 28 mm, operating at the inlet axial Mach number 0.10. These dimensions yield the wavelength/chord ratio of 14 for 2 per revolution distortion (i.e. distortion index $m=2$). The work factor ζ is defined by $\zeta=\Delta V_y/V_R$, in which V_R and ΔV_y are the rotation speed of the rotor and the change in the whirling speed of the flow through it, respectively. The following calculations are for $\zeta=0.5$ and the mean flow approaching axially is considered. The outlet from the stage is assumed to become axially

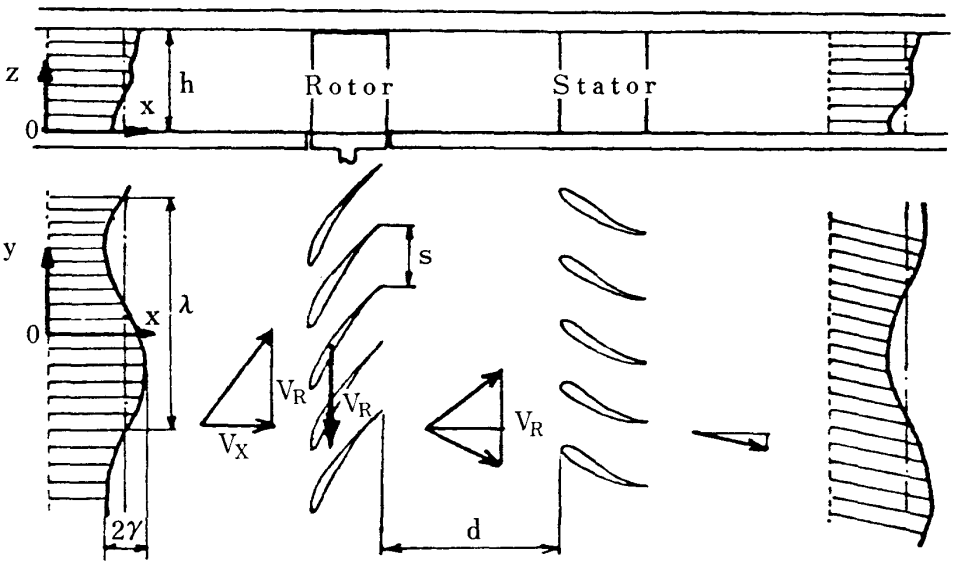

FIG. 2. Test compressor—rotor/stator stage

again. The inlet distortion has been given in a stationary wave form of the axial velocity perturbation; i.e.

$$v_x = -\gamma \cdot \exp\left[i \cdot (2\pi/\lambda) \cdot (z \tan \Phi - y)\right] \tag{16}$$

where, γ and λ are the amplitude and wavelength of the distortion that is skewed in

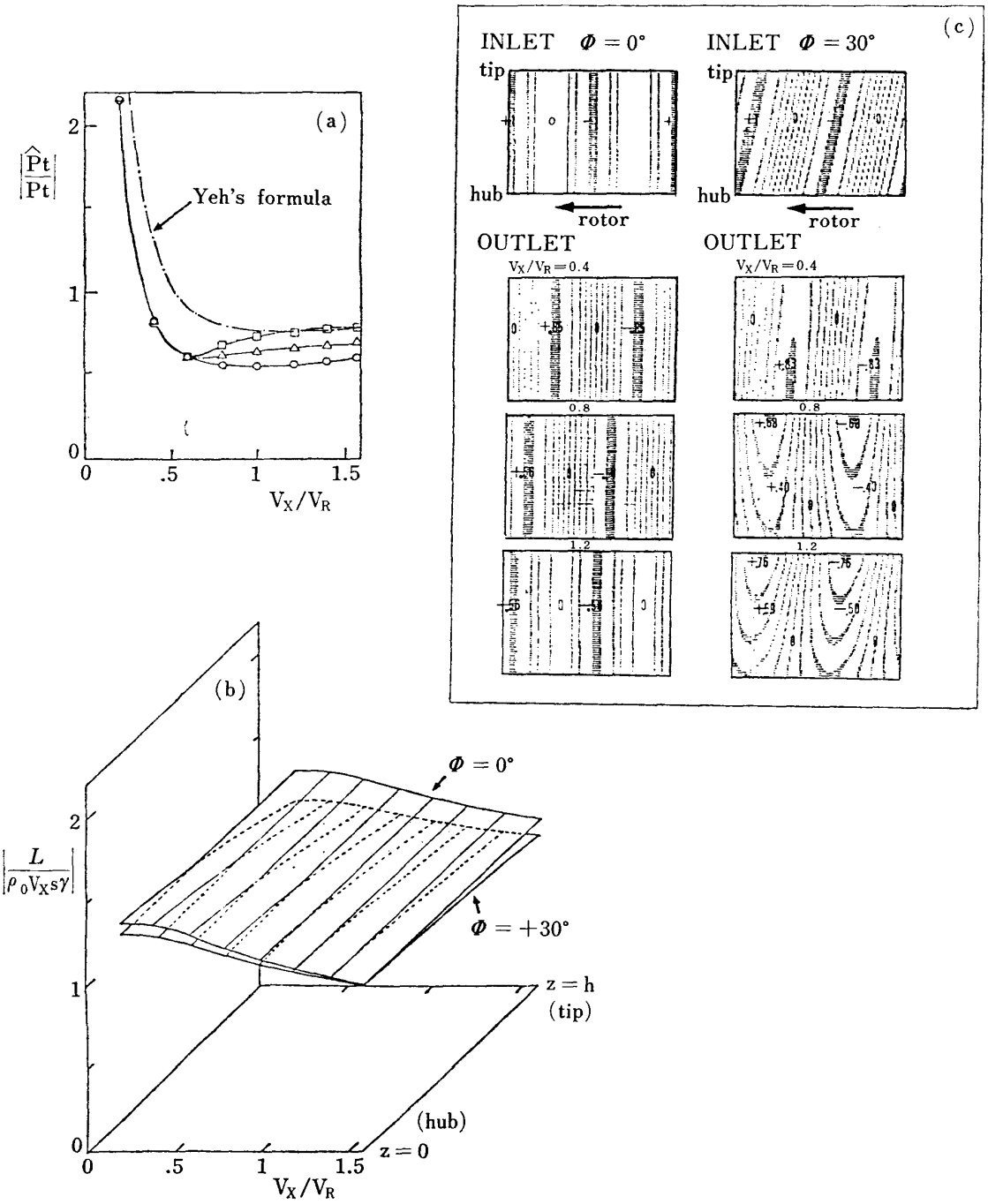

FIG. 3. (a) Distortion induced total enthalpy fluctuation —○— Φ=0°, —△— Φ=±15°, —□— Φ=±30° (b) Unsteady normal force distribution (Φ=0° and +30°), in case of a rigid rotor. (c) Distortion patterns corresponding to three typical values of V_x/V_R.

z-direction by the angle Φ. ($\Phi>0$ towards the y direction) Fig. 3 shows (a) the downstream total enthalpy fluctuation $\widehat{Pt}$ associated with distortion with respect to

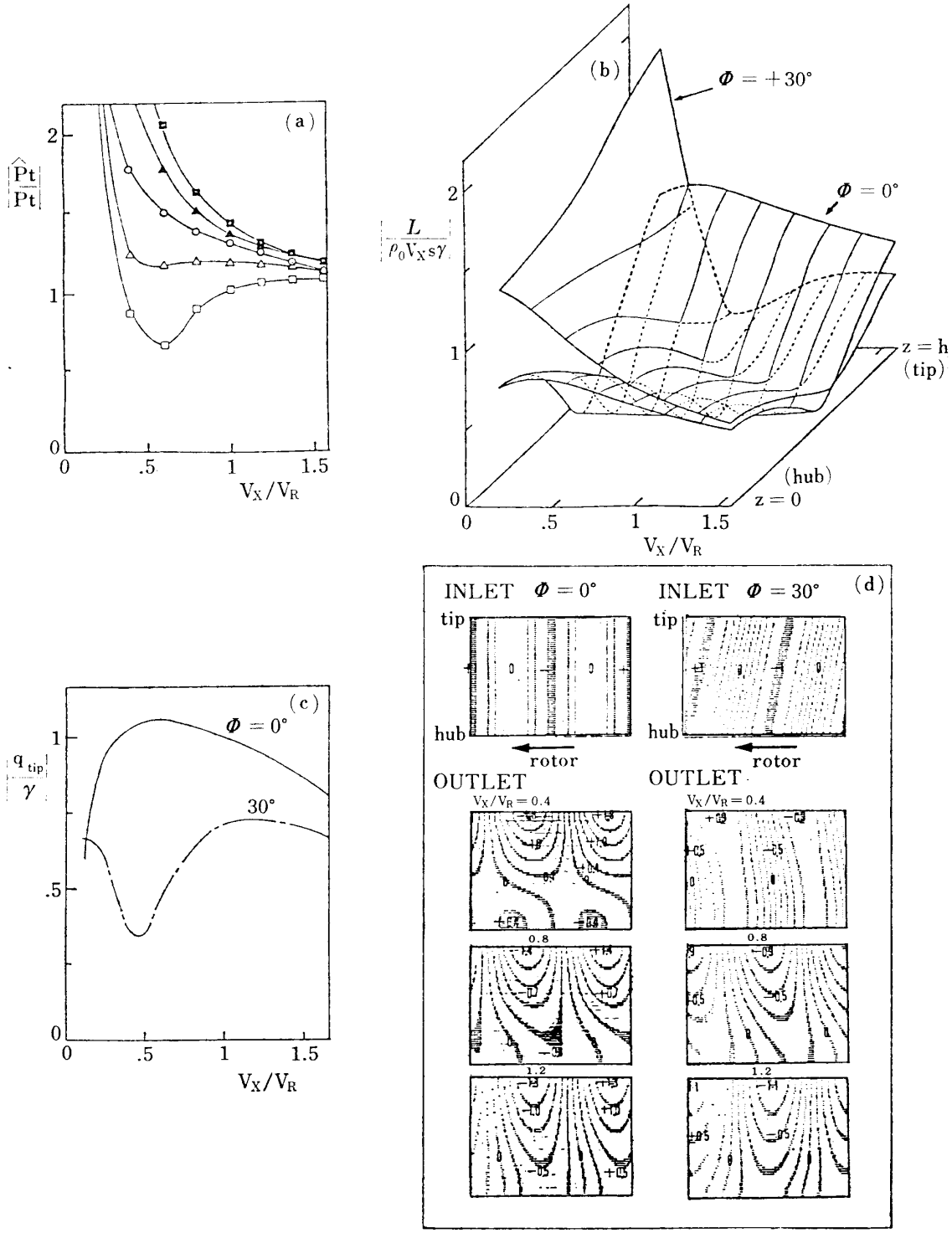

FIG. 4. (a) Distortion induced total enthalpy fluctuation —○— Φ=0°, —△— Φ=+15°, —▲— Φ=−15°, —□— Φ=+30°, —■— Φ=−30° (b) Unsteady normal force distribution (Φ=0° and +30°), when rotor blades are vibrating in resonance with the first bending mode. (c) Amplitude of vibration velocity at the blade tip. (d) Distortion patterns corresponding to three typical values of V_X/V_R.

that of the inlet flow Pt through an isolated rigid rotor (b) the distribution of the modulus of the normal unsteady force L along the blade span against the reciprocal of various rotor speeds V_R, and (c) the outlet distortion patterns at three typical values of V_x/V_R. The unskewed distortion pattern remains to be similar through a rigid rotor except for a lateral shift, since such interaction is of two dimensional structure. On the other hand the skewed distortion emerges as a different pattern according to the rotor operation, since its attenuation varies from hub to tip section. The min-max of the distortion levels has been taken as the ordinate value in the figures. The result according to the Yeh's formula [2, Eq. 34] is also plotted in Fig. 3(a). The present theory predicts better attenuation than the Yeh's. The inlet dis-

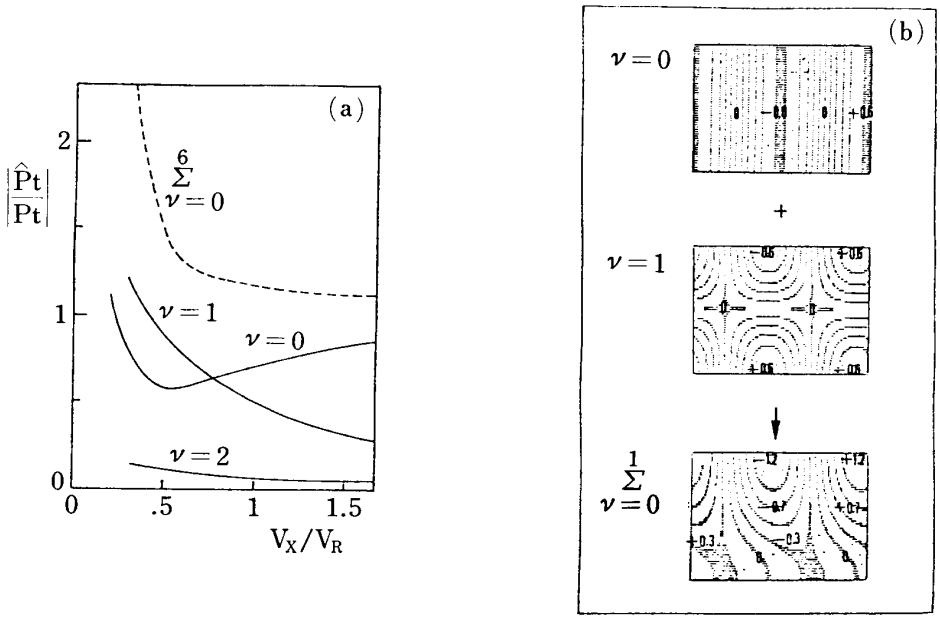

FIG. 5. Modal decomposition of (a) total enthalpy fluctuation and (b) distortion patterns corresponding to $V_X/V_R=0.8$, in case of $\Phi=0°$.

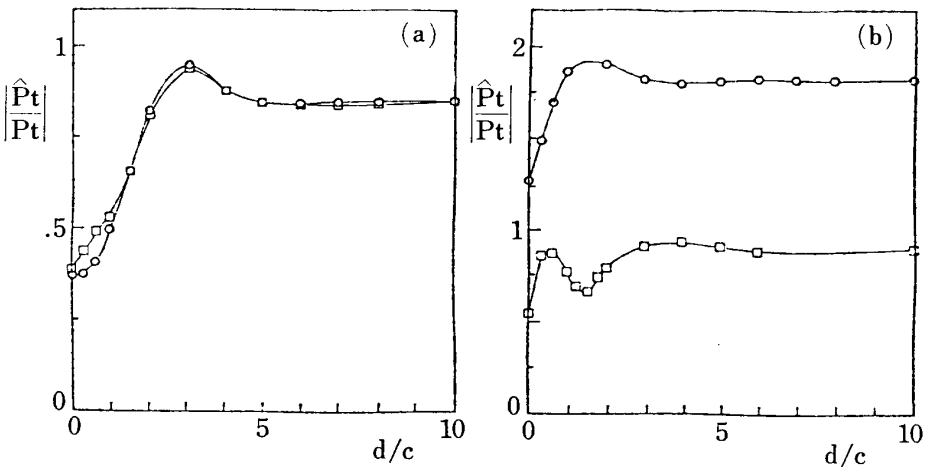

FIG. 6. Effect of rotor/stator separation upon stage attenuation (a) rigid rotor blades (b) rotor blades at resonant vibration —○— $\Phi=0°$, —□— $\Phi=+30°$, distortion index $m=4$ and $V_X/V_R=0.4$.

tortion skew makes that improvement poor as the rotor speed goes down. Backward skew against the rotor revolution ($\Phi>0$) lowers the fluctuating force at the tip section. The corresponding results when the rotor blades are vibrating are shown in Fig. 4. The resonant state of vibration with the n-th bending mode has been assumed and for simplicity the contributions from the other normal modes in the equation (15) are neglected. In the absence of mechanical damping this leads to the balance between the aerodynamic damping force and the exciting force due to inlet distortion, whence the amplitude of vibration velocity $q(z, t)$ can be calculated,

$$q(z, t)=\sum_{\nu} q_{\nu}\cdot\cos[(\pi\nu/h)z]\cdot\exp(i\omega t)$$

where, $q_{\nu}=i\omega\varepsilon_{n}\psi_{n\nu}=-\psi_{n\nu}\sum_{j}(f_{\bar{\omega}j}/f_{qj})\cdot(\bar{\omega}_{j}/\psi_{nj})$ and $\omega_{n}=\omega=(2\pi/\lambda)\cdot V_{R}$. The resulting normal force becomes therefore,

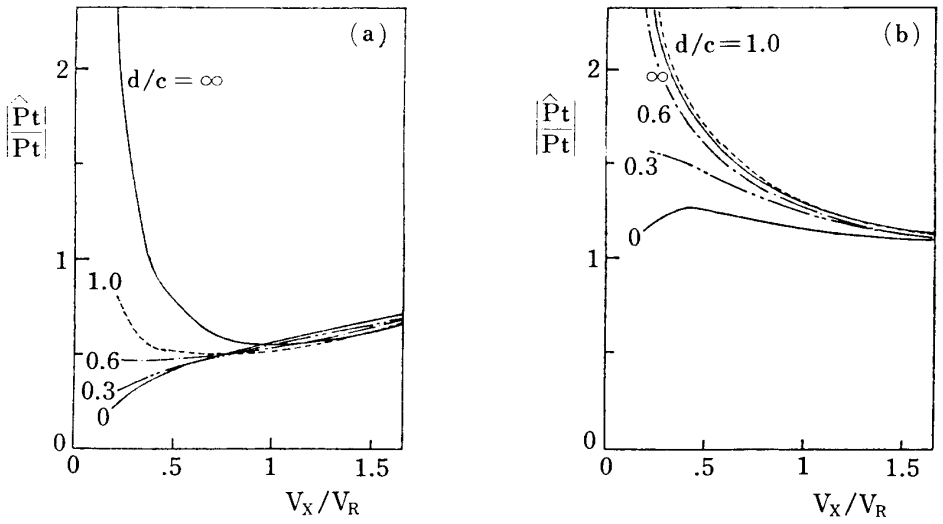

FIG. 7. Effect of rotor/stator separation upon stage attenuation (a) rigid rotor blades (b) rotor blades at resonant vibration, distortion index $m=4$, $\Phi=0°$.

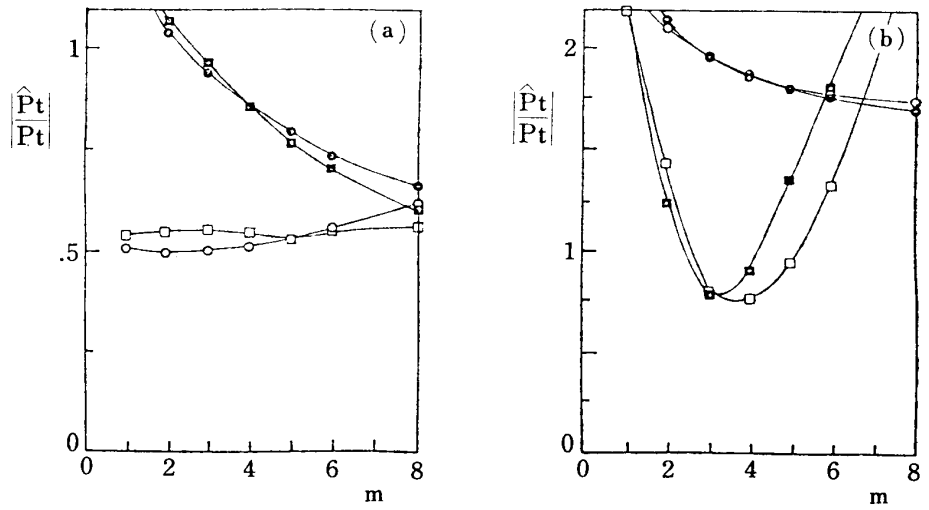

FIG. 8. Effect of distortion index upon stage attenuation (a) rigid rotor blads (b) rotor blades at resonant vibration —○— $\Phi=0$, —□— $\Phi=+30°$, for $d/c=1$; —●— $\Phi=0°$, —■— $\Phi=+30°$, for $d/c=10$; in case of $V_X/V_R=0.4$.

$$L/\rho_0 V_x s = -\sum_{\nu} f_{q\nu}\psi_{n\nu}\cos[(\pi\nu/h)z]\sum_{j\neq\nu}(f_{\bar{\omega}j}/f_{qj})(\bar{\omega}_j/\psi_{nj}) \tag{17}$$

It can be seen from Fig. 4(a) that the vibration gets the distortion worse, distinctly so in cases of forwardly skewed inlet distortion ($\Phi<0$). The rotor speed being about twice of the axial flow velocity, a backward skew seems to be favourable for attenuation. There the fluctuating force at the tip gets almost the minimum value as shown in Fig. 4(b) and the amplitude of vibration velocity at the blade tip section drops correspondingly as shown in Fig. 4(c). In the absence of skew the blade section

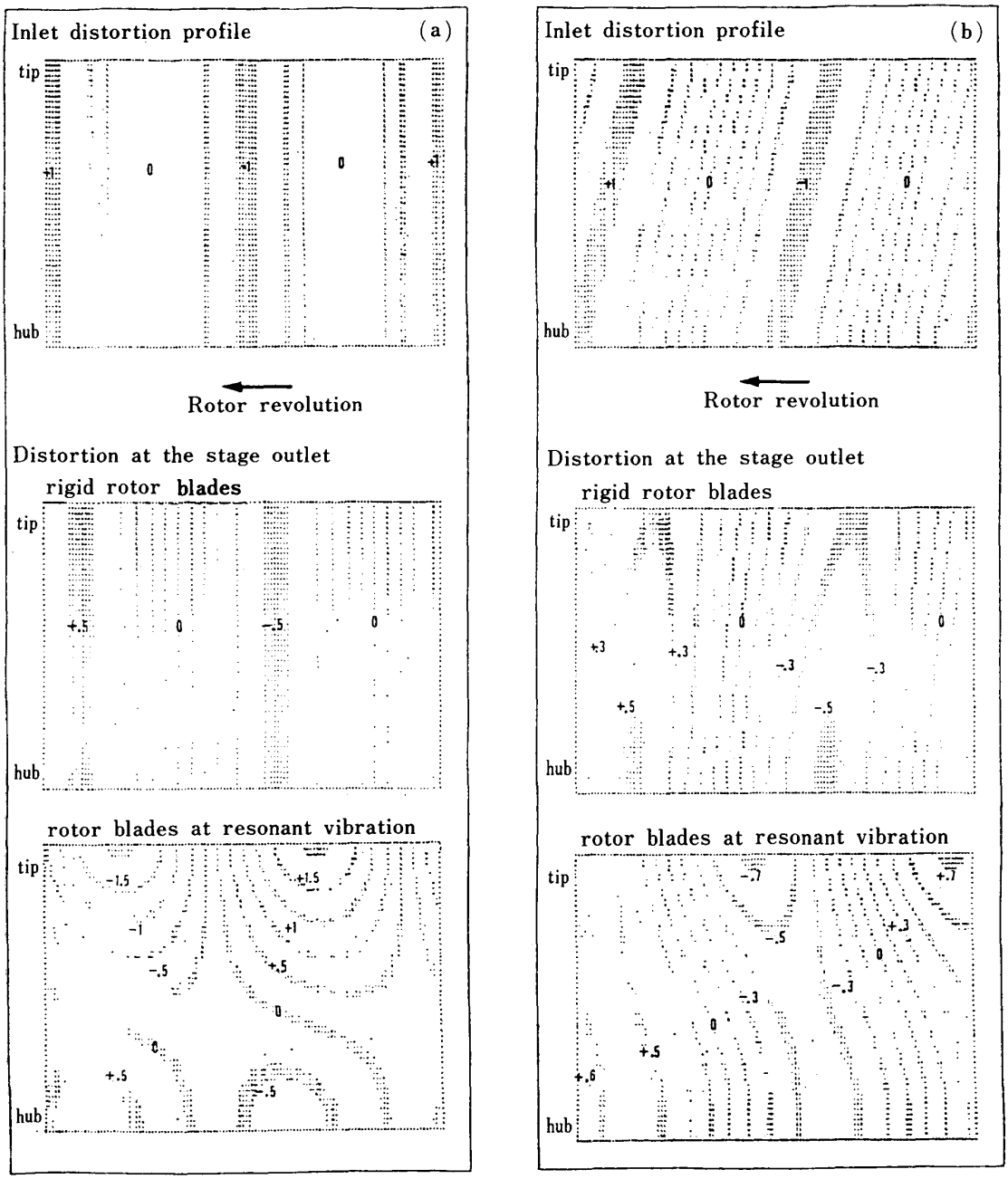

FIG. 9. Inlet and outlet distortion patterns in the cross flow plane viewed from the downstream of the stage (a) $\Phi=0°$ (b) $\Phi=+30°$ for rotor/stator separation $d/c=1$, distortion index $m=4$ and $V_X/V_R=0.4$.

yielding the minimum normal force is located slightly beyond the mid-span, closer, to the tip. According to the two dimensional semi-actuator disc analysis, this force at the resonance is found to be always naught. Outlet distortion patterns for three values of V_x/V_R are also shown in Fig. 4(d), which are obtained by superposing the spanwise modes of the lowest 7 orders. For the inlet distortion without skew the distortion pattern can be approximated by adding the patterns corresponding to the first 2 modes, since the present deflection of a blade can be well described by the leading 2 terms of the spanwise Fourier series expansion and such distortion is hardly likely to produce strong coupling with the higher order modes. An illustration of this is shown in Fig. 5(b) for the case of $V_x/V_R=0.8$ and the corresponding results of modal decomposition are plotted in Fig. 5(a). Fig. 6 shows the effects of rotor/stator separation d/c upon attenuation for $V_x/V_R=0.4$. Without skew a peak value appears at the separation being around 2 or 3 times of the blade chord length. The results, as the rotor operation is varied, are shown in Fig. 7. The skew influences largely upon the results for vibrating rotor blades as seen from Fig. 6(b). The better attenuation is generally expected for the closer packed stage. Fig. 8 shows the effects of circumferential distortion index m for $d/c=1$ and 10. Without skew the larger index yields on the whole better attenuation, but the skew makes this tendency be complex, for instance, the sharp rise of the curve at a blade chord length separation is noticed as the index m increases. The results at large indices m, however, become dubious, since the assumption that the wavelength of distortion be large compared with the blade spacing will then be violated. Fig. 9 concludes the present calculations. It compares the distortion patterns between the inlet and outlet of the given stage. The difference, depending upon whether the rotor blades are vibrating or not, can be clearly observed.

Department of Propulsion
Institute of Space and Aeronautical Science
University of Tokyo
10 December 1980

References

[*1*] F. Ehrich 1957 J. Aeronautical Science **24**, 413–417. Circumferential Inlet Distortions in Axial Flow Turbomachinery.

[*2*] H. Yeh 1959 J. Aeronautical Science **26**, 739–753. An Actuator Disc Analysis of Inlet Distortion and Rotating Stall in Axial Flow Turbomachines.

[*3*] J. Dunham 1962 J. Aeronautical Science **29**, 361–362. Comment on An Actuator-Disc Analysis of Inlet Distortion and Rotating Stall in Axial Flow Turbomachines.

[*4*] Y. Tanida and T. Okazaki 1963 Bulletine of Japan Society of Mechanical Engineers **24**, 744–753. Stall-Flutter in Cascade, I & II.

[*5*] Y. Tanida 1972 J. Applied Mathematics and Physics (ZAMP) **23**, 645–654. Inlet Airflow Distortion in Turbomachinery.